




Research Article

Iranian Qara Qat fruit (redcurrant) in Arasbaran forests as the resource of anthocyanin pigments in formation of [ACN-Mg²⁺/Al³⁺/Ga³⁺/Sn²⁺/Cr³⁺/Fe³⁺] chelation clusters

Fatemeh Mollaamin¹  · Nayer T. Mohammadian² · Narges Najafloou³ · Majid Monajjemi¹

Received: 18 August 2020 / Accepted: 23 February 2021 / Published online: 2 March 2021

© The Author(s) 2021 

Abstract

Clusters of metallic cations (Mg²⁺, Al³⁺, Ga³⁺, Sn²⁺, Cr³⁺ and Fe³⁺) jointed to anthocyanins in water media were studied for unraveling the color shifting of different complexes of these structures in the low ranges of pH. Anthocyanin jointed to metallic cation progresses the color expression range of anthocyanin in more different range of pH. In this verdict, it has been studied the metallic cations diffusing of deprotonating for the anthocyanin (B)-ring of cyanidin (Cy), delphinidin (Dp) and petunidin (Pt) in two media of gas and water, transforming flavylium cations to the blue quinonoidal bases at lower range of pH applying the infrared method by approaching Beer Lambert law for getting the physico-chemical parameters of frequency, intensity, and absorbance of the compounds, respectively. In previous investigation, it has been indicated that the important factor for enhancing the absorbance in a positive non-linear fashion due to deviating from the Beer Lambert law is the self-association of anthocyanins of cyanidin, delphinidin and petunidin of anthocyanin structures. The difference of heat of formation (ΔH_f) among clusters of metallic cations jointed to anthocyanins has been illustrated toward the double bonds and carbonyl groups by the chelation of (B)-ring for cyanidin, delphinidin and petunidin anthocyanins in two media of gas and water that explains the stability and color of [anthocyanin-metallic cations] cluster chelation of cyanidin (Cy), delphinidin (Dp) and petunidin (Pt) colorful pigments in a weak acidic medium. By this work we exhibited that the color of the anthocyanin chelates is an important factor for estimating the efficiency of these types of food colorants.

Keywords Iranian Qara Qat fruit · [anthocyanin-metallic cations of (Mg²⁺, Al³⁺, Ga³⁺, Sn²⁺, Cr³⁺ and Fe³⁺)] cluster chelation · Anthocyanin-metal chelate · Cyanidin (Cy) · Delphinidin (Dp) · Petunidin (Pt)

1 Introduction

The compounds of anthocyanin water soluble and polar derivatives which have a large membrane bound vesicle in a cell's cytoplasm can be seen in different colors in an expanded range of colors such as red, purple, blue or black [1–3]. The aromatic cyclic group of anthocyanins are a part of fundamental compounds as flavonoids synthesized via the phenyl propanoid pathway which are

discovered in roots, stems, leaves, flowers, and fruits. The portion of the most common anthocyanidins in fruits and vegetables including cyanidin, delphinidin, pelargonidin, peonidin, malvidin, and petunidin is 50%, 12%, 12%, 12%, 7%, and 7%, respectively [4]. In nature, cyanidin in berries is a reddish-purple major pigment and other red-colored vegetables such as red sweet potato and purple corn [5, 6]. Delphinidin (Dp) has a chemical characteristic similar to most of the anthocyanidins which appears as a

✉ Fatemeh Mollaamin, smollaamin@gmail.com; ✉ Majid Monajjemi, maj.monajjemi@iauctb.ac.ir | ¹Department of Chemical Engineering, Central Tehran Branch, Islamic Azad University, Tehran, Iran. ²Department of Chemistry, Ardabil Branch, Islamic Azad University, Ardabil, Iran. ³Department of Chemistry, Science and Research Branch, Islamic Azad University, Tehran, Iran.



blue-reddish or purple pigment in the plant like the blue hue of flowers which is due to the delphinidin pigment [7]. But pelargonidin is different from most of the anthocyanidins as a red-colored pigment [8]. Besides, pelargonidin donates an orange hue to flowers and red to some of the fruits and berries [9, 10]. The investigations on foods and plants consisting of antioxidant characteristics have begun toward indicating the multiple data exhibiting their effects in the reduction of risk through chronic sicknesses on the members in the world [11–14].

Fruits and vegetables have the chemical structures linked to health promotions showing several antioxidants like vitamins (C and E), carotenoids and flavonoids and their characteristics including molecular weight, dimensional conformation, biochemical and physical characteristics of these compounds conduct them to react with different points in many live organisms [15–17].

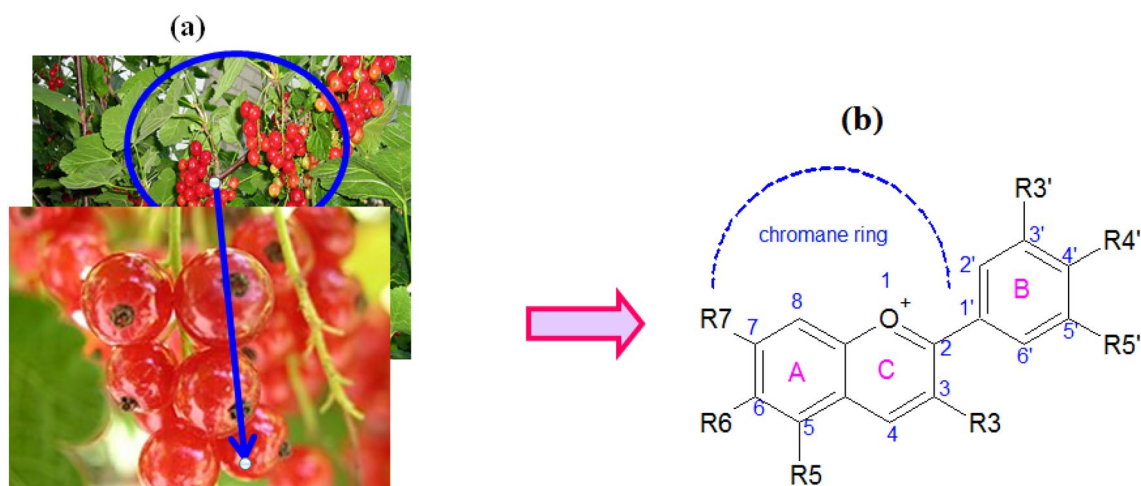
The most advantage of nutrition in anthocyanin pigments through the human life shows the ability of health benefits on various sicknesses like cancer, Alzheimer disease, obesity, neurological diseases, inflammation and diabetes. The compounds of anthocyanin pigments are a big family of polyphenolic molecules as flavonoids that are founded by plants as the part of their secondary metabolism. Flavonoids are divided into different subclasses based on their chemical characteristics and share a popular carbon basis called flavylum ion chain with different rings [18, 19].

The Glycosylated anthocyanidins groups which are linked to the skeleton of anthocyanin have the highest common type of pigments in plants. So, it can be found a variety of anthocyanins due to complex glycosylation models over some aglycones. These compounds are largely colored at low pH, through the eight conjugated double bonds exhibiting a positive charge of the structure

that show various colors due to various substitutions in the aromatic cyclic chains [20–24]. Physicochemical properties of anthocyanin structures are affected by the particle substitutions due to changing the size, polarity and solubility in water toward an expanded range of compounds in nature [25]. It is important how the plants arrange the structure or how chemistry of the anthocyanins produces an expanded range of colors often in the visible spectrum [26]. Moreover, for indicating the color and stability of anthocyanins through the chemical and other photochemical properties, several new anthocyanin-inspired dyes and pigments have been prepared for applying in cosmetics or foods with pleasant colors and stability in comparison to the color and stability of natural anthocyanins [27]. The scientists have explained that the color of natural anthocyanins is sensitive to concentration of hydrogen cation in the solution (weak acidic media are appropriate). Around "pH = 3", changing the color generates the colored anthocyanin cation, AH^+ , which alters into colorless or near-colorless samples (Scheme 1) [28].

Arasbaran vegetation zone is a very rich area in Iran which has most of Iran's herbaceous species including medicinal, ornamental and edible products. Most of the trees in this area are oak, kikem, crimson, barberry, wild pomegranate, wild apples, wild pears and raspberries, and cucumbers, along with fruits called Qara Qat (redcurrant), which is very tasty and sour, and are seasoned in the middle of summer (Scheme 1a). In acidic media, anthocyanin appears as a red pigment while blue pigment anthocyanin appears in alkaline media. Anthocyanin is considered as one of the flavonoids with a positive charge at the oxygen atom of the (C)-ring (Scheme 1b).

Glińska and his coworkers have illustrated the decrease of potential toxic effects of anthocyanins through separating metal cation chelation of these compounds [30]. For



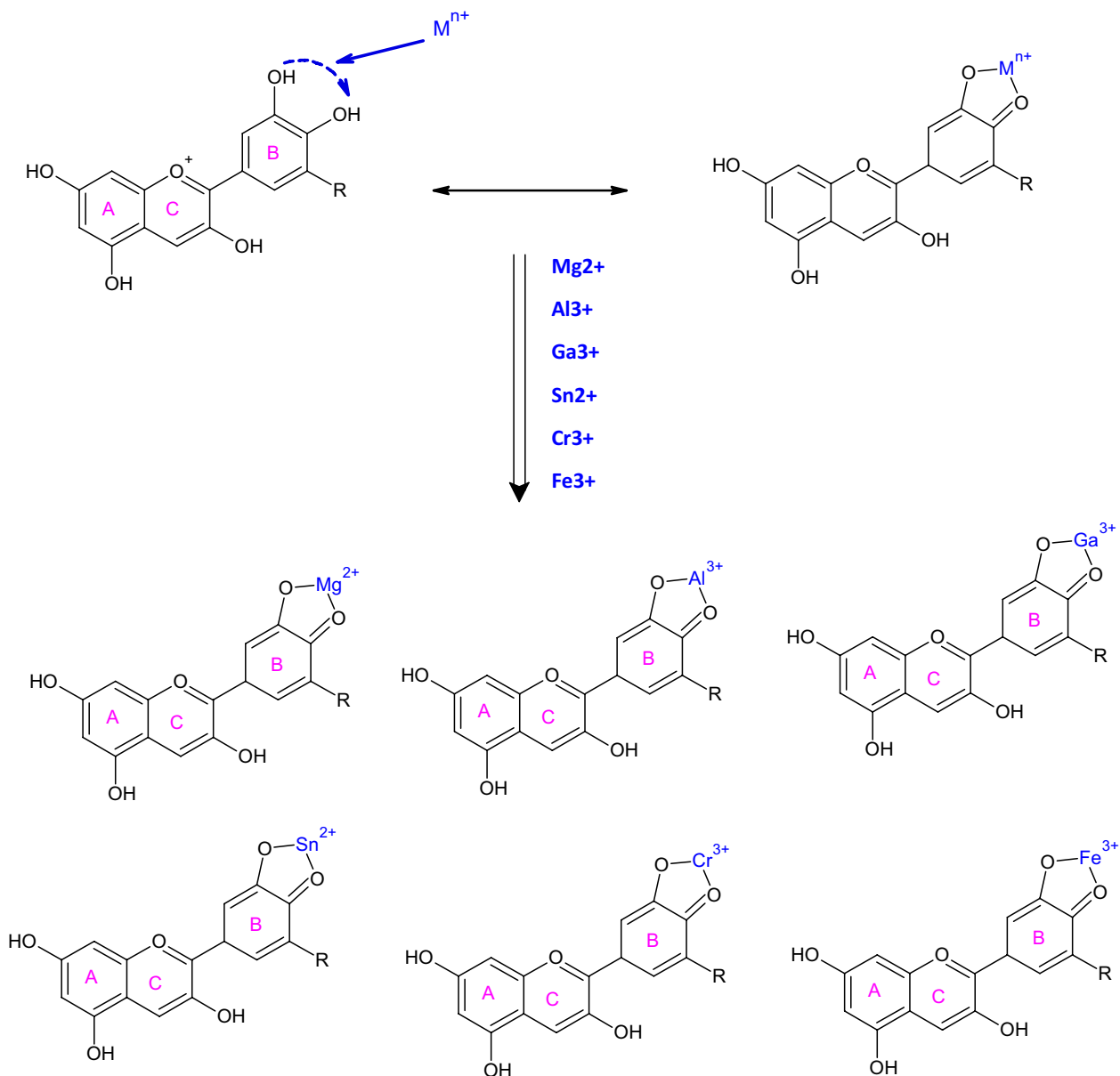
Scheme 1 a Qara Qat fruit (redcurrant) of Arasbaran vegetation in Iran, b Basic anthocyanin structure [28]

being capable of forming metallic cation chelation and expressing purple blue colors, the molecule of anthocyanin must tolerate at least 2 free hydroxyl groups on the (B)-ring. When the cation approaches the anthocyanins, it plays a role to compete with the hydrogen ions for the binding sites (Scheme 2) [31].

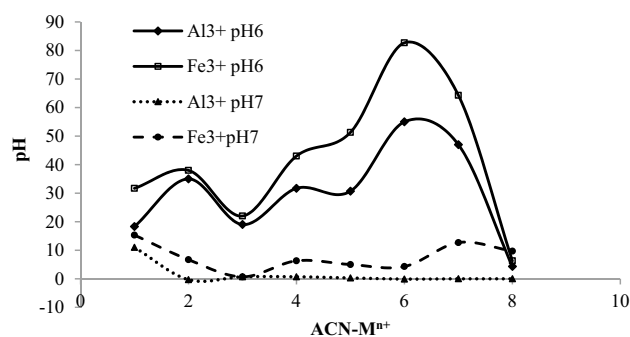
The chelation of (Mg^{2+} , Al^{3+} , Ga^{3+} , Sn^{2+} , Cr^{3+} and Fe^{3+}) metallic cations by cyanidin, delphinidin and petunidin has been more extensively studied due to its relationship with the blue coloration of hydrangea floral compounds. Relatively, stable complexes between delphinidin and aluminum cation have been investigated to form acidified

ethanol and a wide pH range [31]. In these structures, color expression of the delphinidin began red becoming violet and then blue as pH and anthocyanin concentration were maintained, but the aluminum cation content increased. Chelation of aluminum cation with cyanidin has been identified to develop in aqueous samples, pH (2–5) which indicate violet colorations [32].

The spectral responses of these cyanidin complexes jointed to metal cation chelation were more difficult to distinguish in the value of pH 7 (Scheme 3). It has been obvious that large Bathochromic shifts have existed in the value of pH 6, but the appeared changes in maximum λ in



Scheme 2 Pigment clusters of anthocyanin-cation chelation including [anthocyanin-metallic cations of (Mg^{2+} , Al^{3+} , Ga^{3+} , Sn^{2+} , Cr^{3+} and Fe^{3+})] through the (B)-ring for three anthocyanins of Cyanidin, Delphinidin and Petunidin [31]



Scheme 3 The spectral responses of the cyanidin derivatives to metal ion chelation of Al^{3+} & Fe^{3+} in $\text{pH}=7$. Buchweitz and his co-workers compared the stability of aluminum cation chelates of delphinidin-3-rutinoside in American eggplant to that of acylated cyanidin glycosides, red cabbage, as literature is limited about stability of acylated anthocyanin metal chelates

neutral pH were small specially with enhancing metal ion concentrations. Besides, the junction of anthocyanidins to Fe^{3+} cation was a little larger than to aluminum cation based on other investigations. Anthocyanins can gain a maximum amount of λ by these chemical complexes based on the bathochromic replies. Anthocyanin has indicated the maximum value of λ in the range of pH (7, 8) and has showed the hypochromic replies in the higher pH [33, 34].

It has been seen the changes in the observable absorption of the spectra for the colorful pigments existent in solution, but the changes of maximum λ of anthocyanin by metallic cation chelation were small and sometimes negative (Scheme 3).

They explained that anthocyanin metallic complexes are stronger to heat treatment rather than light exposure. Degradation of delphinidin-aluminum chelates seems jointed to concentration with rate decreasing of time, in agreement with recent researches [35].

In the recent researches, it has been approved that aluminum cation in metalloanthocyanins is capable of inducing blue color development with delphinidin, having a pyrogallol moiety on the (B)-ring, but it is not enough to lead to blue colors with cyanidin derivatives [36].

Therefore, a theoretical study of the linkage between the electronic and chemical structure of (Mg^{2+} , Al^{3+} , Ga^{3+} , Sn^{2+} , Cr^{3+} and Fe^{3+}) metallic cations by cyanidin, delphinidin and petunidin and their stability has been followed using theoretical and computational methods in two media of gas and water at 300 K based considering Beer Lambert law for discovering different usages of these structures such as coloring agents in pharmaceutical products and foods. Moreover, it has been illustrated the structural properties of [anthocyanin-metallic cations of (Mg^{2+} , Al^{3+} , Ga^{3+} , Sn^{2+} , Cr^{3+} and Fe^{3+})] cluster chelation in Iranian

Qara Qat fruit by quantum chemical methodologies as the computational design and the simulated class to estimate the physicochemical characteristics of these chelated pigments with metal ions through conserving their stability and color tide.

2 Perspective of cluster chelation

The chelation of anthocyanins of cyanidin, delphinidin and petunidin with (Mg^{2+} , Al^{3+} , Ga^{3+} , Sn^{2+} , Cr^{3+} and Fe^{3+}) metallic cations in Iranian Qara Qat fruit has been studied in this investigation by forming relatively stable complexes in the weak acidified medium with a different pH range. Thus, a series of quantum theoretical approaches has been done for finding the optimized coordination of [anthocyanin-metallic cations of (Mg^{2+} , Al^{3+} , Ga^{3+} , Sn^{2+} , Cr^{3+} and Fe^{3+})] cluster chelation in Iranian Qara Qat fruit with IR computations and following the Beer Lambert Rule using Gaussian09 program package [37].

It has been declared that polarization functions into the applied basis set in the computation always introduce us an important achievement on the modeling and simulation theoretical levels. Normal mode accomplishment is the verdict of harmonic potential wells by analytic methods which maintain the motion of all atoms at the same time in the vibration time scale leading to a natural explanation of molecular vibrations [38–43].

First, optimized geometry coordination of [cyanidin-metallic cations of (Mg^{2+} , Al^{3+} , Ga^{3+} , Sn^{2+} , Cr^{3+} and Fe^{3+})] cluster chelation in Iranian Qara Qat fruit (Fig. 1) through their (B)-ring in two media of gas and water at 300 K have been evaluated in Table 1.

Besides, charge electron transfer and thermodynamic properties of [anthocyanin-metallic cations of (Mg^{2+} , Al^{3+} , Ga^{3+} , Sn^{2+} , Cr^{3+} and Fe^{3+})] cluster chelation in Iranian Qara Qat fruit through their (B)-ring in two media of gas and water at 300 K have been evaluated and compared to each other by different concentration of H^+ in a simulated solvent model (Fig. 2).

In this work, the data have been achieved from thermodynamic parameters of ΔG , ΔH and ΔS for the solute–solvent model of [anthocyanin-metallic cations of (Mg^{2+} , Al^{3+} , Ga^{3+} , Sn^{2+} , Cr^{3+} and Fe^{3+})] cluster chelation in Iranian Qara Qat fruit. The solved data at 300 K have been analyzed compared to gas phase.

Therefore, for accomplishing a stable structure of [anthocyanin-metallic cations of (Mg^{2+} , Al^{3+} , Ga^{3+} , Sn^{2+} , Cr^{3+} and Fe^{3+})] cluster chelation of cyanidin, delphinidin, and petunidin of colorful pigments in Iranian Qara Qat fruit, geometry optimization plus frequency calculations were done; the frequency and intensity of the vibrational modes were calculated with the quantum mechanics of

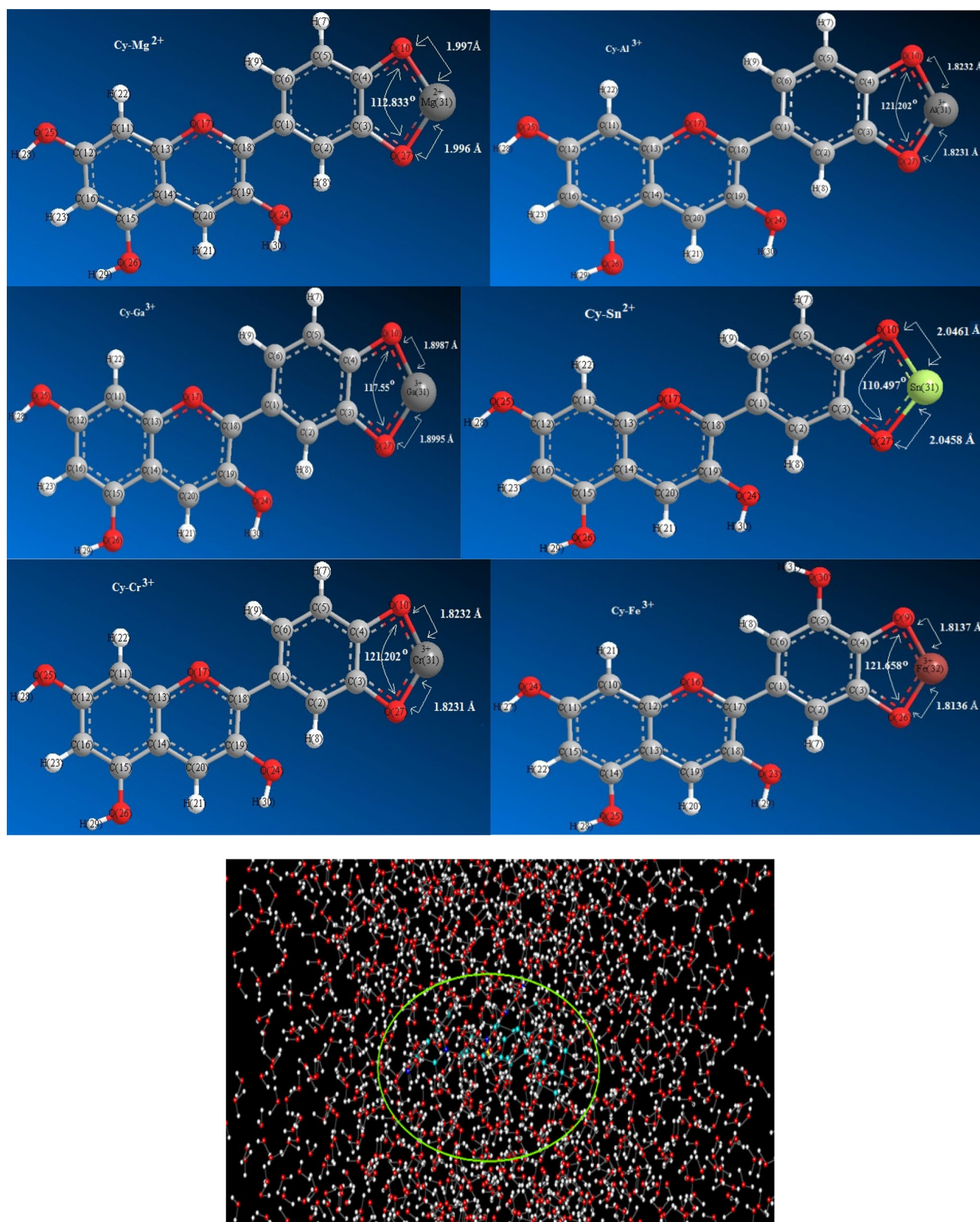


Fig. 1 The schematics of ab initio optimized coordination [anthocyanin-metallic cations of (Mg²⁺, Al³⁺, Ga³⁺, Sn²⁺, Cr³⁺ and Fe³⁺)] through representing the bond length of oxygen-Mⁿ⁺ and bond angle of oxygen-Mⁿ⁺-oxygen calculated by m062x/cc-pvdz

pseudo=lanl2 in solvation optimized with QM/MM model of anthocyanins' family inside 500 water molecules as solvent, including 3 levels of m06-HF for the high (H) layer, Pm3MM semi empirical for the medium and Monte Carlo for low layers at 300 K

Table 1 Optimized geometry with m062x/cc-pvdz pseudo = lanl2 for various [anthocyanin-metallic cations of (Mg^{2+} , Al^{3+} , Ga^{3+} , Sn^{2+} , Cr^{3+} and Fe^{3+})] cluster chelation in Iranian Qara Qat fruit extracted of Fig. 1

Cyanidin-metal ion chelate	Bond length	(Å)	Bond angle	θ°
Cy- Mg^{2+}	O(10)– Mg^{2+} (31)	1.997	O(10)– Mg^{2+} (31)–O(27)	112.833
	Mg^{2+} (31)–O(27)	1.996		
Cy- Al^{3+}/Cr^{3+}	O(10)– Al^{3+}/Cr^{3+} (31)	1.8232	O(10)– Al^{3+}/Cr^{3+} (31)–O(27)	121.202
	Al^{3+}/Cr^{3+} (31)–O(27)	1.8231		
Cy- Fe^{3+}	O(9)– Fe^{3+} (32)	1.8137	O(10)– Fe^{3+} (31)–O(27)	121.658
	Fe^{3+} (32)–O(26)	1.8136		
Cy- Ga^{3+}	O(10)– Ga^{3+} (31)	1.8987	O(10)– Ga^{3+} (31)–O(27)	117.55
	Ga^{3+} (31)–O(27)	1.8995		

theoretical method, and the principal vibrational modes were analyzed by their changes of Gibbs free energy in water compared to water medium at 300 K. Thermochemistry analysis follows the frequency and normal mode data. The zero-point energy output in Gaussian-09 has been expanded and corrected as: thermal correction to energy, thermal correction to enthalpy and thermal correction to the Gibbs free. In addition the total energies can be calculated as: sum of electronic and zero point energies, sum of electronic and thermal energies, sum of electronic and thermal enthalpies and sum of electronic and thermal Gibbs free energies. The theoretical calculations were done at various levels of theory to gain the more accurate equilibrium geometrical results and IR spectral data for each of the identified compounds. It is supposed that an additional diffuse and polarization functions into the basis set applied in the computation conduct us to the magnificent progress on the results of theoretical methods. The simulation indicates the approaches which produce a common template of a model at a special temperature by computing all physicochemical properties among the partition function [39].

3 Computational details

In this work, molecular dynamics, (MD), methods produce a series of time-correlated points in phase space in propagating a starting set of coordinates and velocities according to Newton's second equation by a series of finite time steps on [anthocyanin-metallic cations of (Mg^{2+} , Al^{3+} , Ga^{3+} , Sn^{2+} , Cr^{3+} and Fe^{3+})] cluster chelation in Iranian Qara Qat fruit. Unlike single point and geometry optimization calculations, molecular dynamics calculation account for thermal motion (Fig. 3). Molecular dynamics (MD) includes conformation theories, thermodynamic parameters and movement rules of the molecular machine and kinetic energy to the potential energy surface. If a set of initial situations is explained, then Newton's rules cause the molecular machine to raise a path that is indicated as the

molecular dynamics path. This path climbs the potential level in ways that are of important interest to unravel. Both the final point of a path and the trajectory taken to get there are of credit in molecular modeling.

Molecular dynamics simulations, MD, estimate the future velocities and positions of atoms on the basis of their current velocities and positions. At first, the simulation identifies the force on an atom, F_i , as the function of time, toward a negative gradient of the potential energy (Eq. 1);

$$F_i = -\partial V / \partial r_i, \quad (1)$$

V = function of potential energy and r_i is the position of atom i . Then, we can distinguish the acceleration, a_i , of an atom by dedicating the force action to it by the atom mass (Eq. 2);

$$a_i = F_i / m_i. \quad (2)$$

The variety of velocities, v_i , is the integral of acceleration over time. The variation in the position, r_i , is the integral of velocity over time. Kinetic energy, K , is determined as the velocities of the atoms (Eq. 3) [44, 45];

$$K = 1/2 \sum_{i=1}^N m_i v_i^2. \quad (3)$$

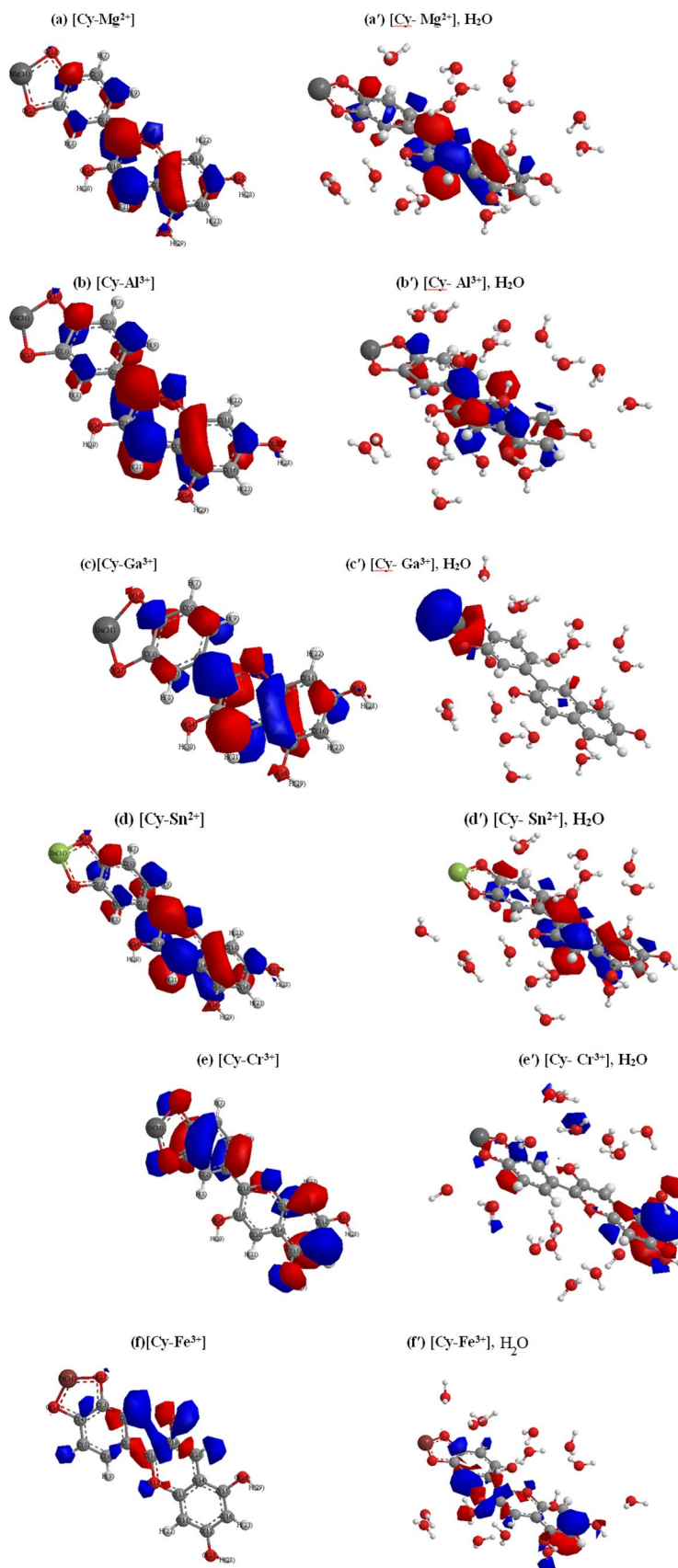
The total energy of the system, called the Hamiltonian, is the sum of the kinetic and potential energies (Eq. 4);

$$H(r, p) = K(p) + V(r) \quad (4)$$

where r is the set of Cartesian coordinates and p is the momenta of the atoms.

The spectral patterns of [cyanidin-(Mg^{2+} , Ga^{3+} , Sn^{2+} , Cr^{3+} and Fe^{3+})] metallic cations] are shown in Fig. 4. The control patterns of these complexes were characterized by two peaks at 280 nm and 520 nm and their spectral intensities were significantly changed. A significant decrease at 520 nm and a significant increase at 280 nm, in a sequence of [cyanidin-($Ga^{3+} > Mg^{2+} > Cr^{3+} > Fe^{3+}$)] were observed.

Fig. 2 Solvation optimized of [anthocyanin-metallic cations of (Mg^{2+} , Al^{3+} , Ga^{3+} , Sn^{2+} , Cr^{3+} and Fe^{3+})] in Iranian Qara Qat fruit with QM/MM model of anthocyanins' family in gas phase (left side) and inside water box periodic box (right side) as solvent model of three stages of m06-HF for the high (H) layer, Pm3MM semi empirical for the medium and Monte Carlo for low layers at 300 K



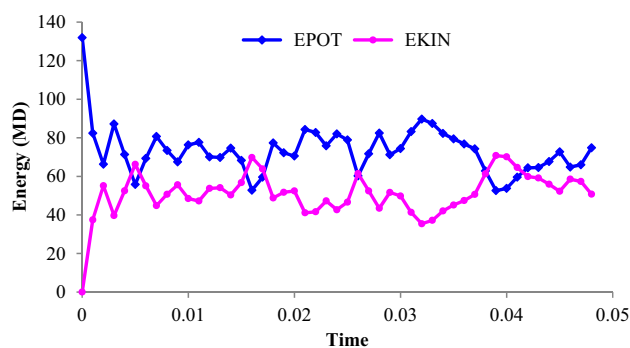


Fig. 3 Optimized energy of anthocyanin-cation metal chelation in Iranian Qara Qat fruit

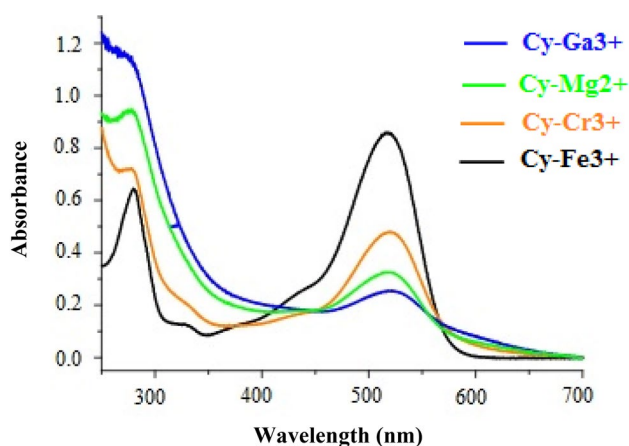


Fig. 4 The effects of metal chelation on the UV-Vis spectral characteristics of cyaniding- M^{n+} ($M=Mg^{2+}$, Fe^{3+} , Al^{3+} , Ga^{3+}) in Iranian Qara Qat fruit

It has been obvious that each site of the complexes including cyanidin- $[Mg^{2+}$, Al^{3+}/Cr^{3+} , Fe^{3+} , $Ga^{3+}]$ have been minimized by ab-initio method via (DFT), density functional theory, which consists of ECP calculations with theoretical levels of lan11, lan12 basis sets and pseudo key due to the metal elements. Besides, those structures have been estimated via QM/MM complex method using an ONIOM level. In our study, the varieties of theoretical methods are discussed due to comparing density and energies with two approaches of "OPLS" and "AMBER" via Monte Carlo (MC) optimization. Moreover, a hyperchem professional (7.01) program pancake has been used for some extra keywords such as "PM3MM" and "PM6" which is pseudo=lan12.

The density function method (DFT) with the "van der Waals" densities functional was illustrated due to modeling of solvent compounds interactions. All minimizations of solvent effects were done by Gaussian09 package. The corrected results were calculated using the theoretical levels of "m062x", "m06-L", and "m06" for chelation of cyanidin

metallic cation effect. The "m062x", "m06-L" and "m06-HF" methods have a suitable correlation in non-bonded calculations between these structures and solvent molecules. The ONIOM theoretical levels have been performed through three levels of high "H", medium "M" and low "L" calculations which The density function method (DFT) methods were applied for the high "H" layer and the semi empirical method of "PM6" and "PM3MM" was applied for the medium and finally Monte Carlo (MC) for low layers, respectively.

The Polarizable Continuum Model, "PCM", is the most popular "SCRF" model based on apparent surface charges diffusing to discuss non-electrostatic impacts with scaled point theory [46, 47].

Kirkwood developed [48, 49] the most common levels of the "SCRF" method of multiple expansions with an algorithm based on the use of a strict multipolar expansion up to the 7th order by Frisch that is currently available at both semi-empirical and ab initio levels of theory.

Onsager [50] and have arranged an intention for various continuum solvation examples of a multiple expansion, "MPE", of the solute charge distribution [51]. Then, Wiberg and co-workers improved Onsager-SCRF for the Gaussian program [52].

Solvation is illustrated in terms of a dipole moment with an iterative path of quantum mechanics calculations on the structure. The perspective of Onsager-SCRF was one to directly apply almost all of the computational characteristics of Gaussian program. The dielectric continuum models like the self-consistent reaction field approach are efficient in applying account the long range of solute-solvent electrostatic interactions and the effect of solvent polarization. Another theoretical level is combination of molecular mechanics (MM) solvent molecule with quantum mechanics level (QM) for electronic structure of the solute molecule named "QM/MM" which can modify deficiency of the dielectric continuum model [53, 54].

Absorbance is a direct measure of how much light is absorbed by our samples in this work. As the absorbance can take on values between 0 (at 100% Transmittance) and about 2.0 (at 1% Transmittance); thus large values of absorbance are associated with very little light passing entirely through the sample and small values of absorbance are associated with most of the light passing entirely through the samples. We could imagine two interesting situations. First one, if we pass a beam of light of the appropriate wavelength through a fairly dilute solution, second, we could imagine that the photons will encounter a small number of the absorbing by the metal ions of chemical species such as metallic cations of (Mg^{2+} , Al^{3+} , Ga^{3+} , Sn^{2+} , Cr^{3+} and Fe^{3+}), so we might expect a high % transmittance and a low absorbance. Alternatively, if we pass the same beam of light

through a highly concentrated solution, we could imagine that the photons will encounter a large number of the absorbing chemical species including [anthocyanin-metallic cations of (Mg^{2+} , Al^{3+} , Ga^{3+} , Sn^{2+} , Cr^{3+} and Fe^{3+})].

In this article, the light goes due to a number of molecules as the system, the anthocyanidin pigments appear the spectrum of molecular transformations with the pH varieties, and generating variation in colors; (1) (Flavylium cation) $pH > 3$ red, (2) Carbonyl pseudo base ($pH = 4-5$ colorless), (3) the hydro base ($pH = 6-7$ violet), (4) an-hydro base anion ($pH = 7-8$ blue), (5) chalcone ($pH > 8$ yellow)", therefore $\frac{I_0}{I_1} = \frac{I_2}{I_3} + \frac{I_3}{I_4} + \frac{I_4}{I_5} = n$. This qualitative relationship is defined by a function for light intensity: $I_i = I_0 n^{-i}$ or $I_i = 10^{-i \log_{10} n}$ which "i" is a number of species in the mechanism. The final expression might be normalized for each system with light path-length (l): $I = I_0 10^{-kl}$, which k is the coefficient depending on concentration, c, and the molar absorptivity, ϵ : consequently, $k = \epsilon \times c$ (Scheme 4).

A Hyperchem model has been applied for calculation the pH [Scheme 5] using a box via various dimensions including N molecules H_3O^+ . The volume (V) of each box has been yielded by multiple of $V = a \times b \times c$ and the pH has been calculated via concentration of $[H^+] = N/V$ with $pH = -\log [H^+]$.

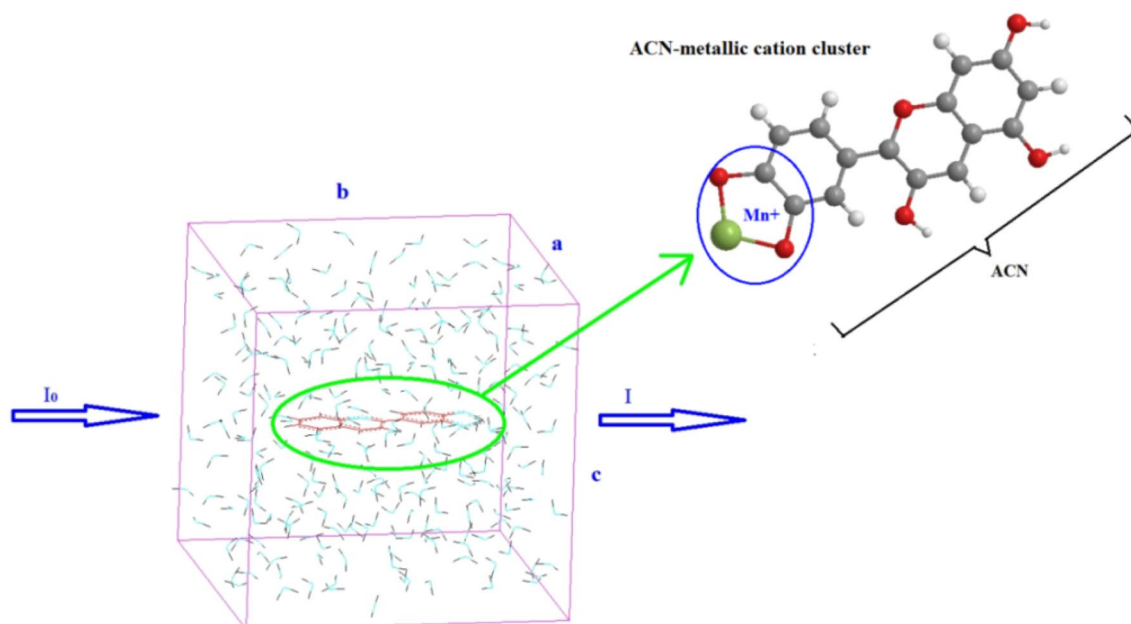
4 Results and discussion

In this project, three anthocyanin pigments of cyanidin (Cy), delphinidin (Dp), and petunidin (Pt) have been estimated using theoretical methods to measure the effect of metal chelation of different plants including factorial excess of metallic cations of (Mg^{2+} , Al^{3+} , Ga^{3+} , Sn^{2+} , Cr^{3+} and Fe^{3+}) in different pH and evaluated by IR spectroscopy using Gaussian09 in two media of gas and water at 300 K (Figs. 1, 2).

The thermodynamic properties of ΔG , ΔH , ΔS , Electronic Energy and Core-Core Interaction, frequency spectrums, anthocyanin concentration, and pH determined final color and intensity (Table 2 and Fig. 5a, b) [37, 55]. The difference of ΔH_R among [anthocyanin-metallic cations of (Mg^{2+} , Al^{3+} , Ga^{3+} , Sn^{2+} , Cr^{3+} and Fe^{3+})] cluster chelation in Iranian Qara Qat fruit (Fig. 5b) has been unraveled due to double bonds and carbonyl groups through the chelation of (B)-ring for Cy, Dp and Pt anthocyanins in two media of gas and water.

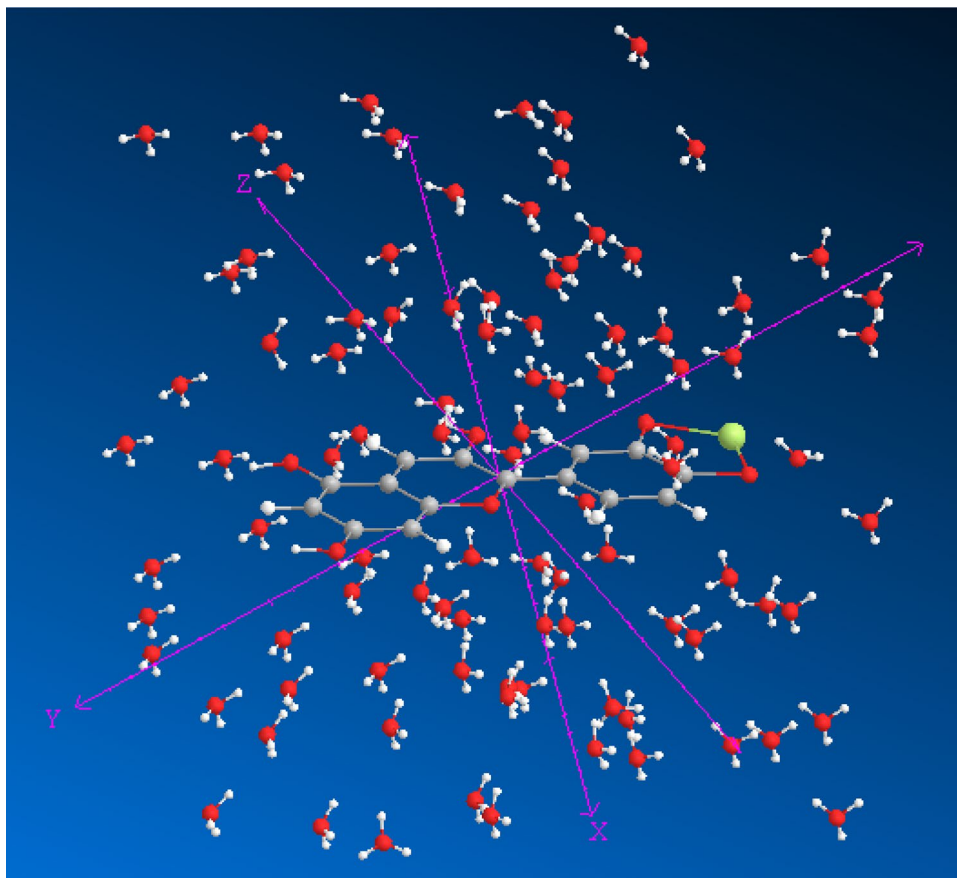
They have been illustrated the stabilities and color of [anthocyanin-metallic cations of (Mg^{2+} , Al^{3+} , Ga^{3+} , Sn^{2+} , Cr^{3+} and Fe^{3+})] cluster chelation of Cy, Dp, and Pt pigments in Iranian Qara Qat fruit in a weak acidic condition (Figs. 1, 2).

The highest chelate stability with different ACNs indicates that ACN-metal chelation can produce a variety range of colors under acidic pH with efficiency for food consume. The results of ΔH_R for formation of



Scheme 4 The relation of light intensity in the Beer Lambert law with concentration aspect of metal ion chelation of anthocyanin's family like anthocyanin- M^{n+} , in water in Iranian Qara Qat fruit

Scheme 5 The 112 number of H_3O^+ around the Cy-Sn in a box with dimension $a=15$, $b=15$ and $c=15$ angstrom for calculation the concentration of $[\text{H}^+]$ and also estimating of the related pH



[anthocyanin-metallic cations of (Mg^{2+} , Al^{3+} , Ga^{3+} , Sn^{2+} , Cr^{3+} and Fe^{3+})] cluster chelation have been extracted by Fig. 5b and data of Tables 2 and 3.

Recently, Beer Lambert law has been used for optimized compounds of [anthocyanin-metallic cations of (magnesium, aluminum, gallium, tin, chrome and iron)] cluster chelation in Iranian Qara Qat fruit to demonstrate the absorbance of assigned molecules toward showing the stabilization and a range of color due to their electronic structures in H_2O medium with different concentrations of H^+ [55–57]. The absorbance (A) of the [anthocyanin-metallic cations of (magnesium, aluminum, gallium, tin, chrome and iron)] of cyanidin, delphinidin, and petunidin colorful pigments in Iranian Qara Qat fruit in H_2O periodic box of a simulated model has been calculated through the Beer Lambert law which directly depends on concentration ($c/\text{mol/L}$) of H^+ . The results have been shown in [55–57] based on basic equations of $A = \log_{10} (I_0/I) = \epsilon lc$, where A is the absorbance; I , intensity of light; ϵ , molar absorptivity coefficient and c , concentration of solution. Basically, the increase in absorbance continued to rise with increasing and decreasing of frequency (F) for anthocyanin-metal cation chelation of cyanidin- Al^{3+} and petunidin- Al^{3+} in higher pH, respectively.

These decreases in absorbance could be related to decreased solubility of the anthocyanin- M^{n+} -cluster chelation which is resulted in precipitation of some complexes. In neutral or alkaline pH, hyper-chromic effects were found to be highest with much lower M^{n+} levels; they were largest in higher pH with M^{n+} and [anthocyanin], respectively, and were pursued by absorbance decreases. The large increases in absorbance could be treated to convert as the colorless forms of ACN to those which absorb and reflect visible light as well as the M^{n+} induced linked to anthocyanin compounds.

So, it has been shown the Changes of absorbance (A) versus concentration (c) through Beer Lambert law for [cyaniding-metallic cations of (Mg^{2+} , Al^{3+} , Ga^{3+} , Sn^{2+} , Cr^{3+} and Fe^{3+})] chelation and [petunidin-metallic cations of Mg^{2+} , Al^{3+} , Ga^{3+} , Sn^{2+} , Cr^{3+} and Fe^{3+})] cluster chelation in the weak acidic media by different concentrations of H^+ at 300 K [55–57].

There is a high tendency to the absorbance of Cy, Dp and Pt with Mg^{2+} added, but the changes were of small magnitude by playing a role in organizing ACN into supra-molecular assembly similar to the role of Mg^{2+} , which plays in metalloanthocyanins formation [36].

Mg^{2+} is the only divalent metal cation used in this work which is a crucial M^{n+} to life system and usually linked to

Table 2 Thermodynamic properties of (Mg^{2+} , Al^{3+} , Ga^{3+} , Sn^{2+} , Cr^{3+} and Fe^{3+}) metallic cation chelation for cyanidin, delphinidin, petunidin pigments in two media of gas(g) and water (w) at 300 K, calculated by m062x/cc-pvdz pseudo = lanl2

Pigment-metal chelation	ΔG (kcal/mol)	ΔH (kcal/mol)	ΔS (kcal/K-mol)	$E_{\text{electronic}}$ (kcal/mol)	$E_{\text{core-core}}$ (kcal/mol)
Cy- Mg^{2+} (g)	-8.52×10^4	-4.57×10	2.84×10^2	-5.33×10^5	4.47×10^5
Cy- Mg^{2+} (w)	-2.27×10^5	-1.08×10^3	7.55×10^2	-2.21×10^6	1.98×10^6
Dp- Mg^{2+} (g)	-9.20×10^4	-8.49×10	3.06×10^2	-5.83×10^5	4.91×10^5
Dp- Mg^{2+} (w)	-2.19×10^5	-1.03×10^3	7.28×10^2	-2.05×10^6	1.83×10^6
Pt- Mg^{2+} (g)	-9.54×10^4	-7.12×10	3.18×10^2	-6.33×10^5	5.38×10^5
Pt- Mg^{2+} (w)	-2.15×10^5	-9.70×10^2	7.14×10^2	-2.05×10^6	1.83×10^6
Cy- Al^{3+} (g)	-8.58×10^4	-8.33×10	2.86×10^2	-5.40×10^5	4.54×10^5
Cy- Al^{3+} (w)	-2.28×10^5	-1.05×10^3	7.57×10^2	-2.22×10^6	1.99×10^6
Dp- Al^{3+} (g)	-9.26×10^4	-1.25×10^2	3.08×10^2	-5.91×10^5	4.98×10^5
Dp- Al^{3+} (w)	-2.20×10^5	-1.00×10^3	7.30×10^2	-2.07×10^6	1.85×10^6
Pt- Al^{3+} (g)	-9.60×10^4	-1.12×10^2	3.20×10^2	-6.41×10^5	5.45×10^5
Pt- Al^{3+} (w)	-2.16×10^5	-9.40×10^2	7.16×10^2	-2.07×10^6	1.85×10^6
Cy- Ga^{3+} (g)	-8.60×10^4	-1.63×10	2.86×10^2	-5.41×10^5	4.55×10^5
Cy- Ga^{3+} (w)	-2.28×10^5	-1.05×10^3	7.57×10^2	-2.22×10^6	1.99×10^6
Dp- Ga^{3+} (g)	-9.28×10^4	-5.53×10	3.09×10^2	-5.92×10^5	4.99×10^5
Dp- Ga^{3+} (w)	-2.20×10^5	-1.02×10^3	7.30×10^2	-2.07×10^6	1.85×10^6
Pt- Ga^{3+} (g)	-9.63×10^4	-9.61×10	3.20×10^2	-6.42×10^5	5.46×10^5
Pt- Ga^{3+} (w)	-2.23×10^5	-1.02×10^3	7.42×10^2	-2.19×10^6	1.96×10^6
Cy- Sn^{2+} (g)	-8.66×10^4	-8.36×10	2.88×10^2	-5.47×10^5	4.61×10^5
Cy- Sn^{2+} (w)	-2.29×10^5	-1.07×10^3	7.59×10^2	-2.24×10^6	2.01×10^6
Dp- Sn^{2+} (g)	-9.33×10^4	-8.29×10	3.11×10^2	5.05×10^5	-5.99×10^5
Dp- Sn^{2+} (w)	-2.21×10^5	-1.02×10^3	7.32×10^2	-2.08×10^6	1.86×10^6
Pt- Sn^{2+} (g)	-9.67×10^4	-5.71×10	3.22×10^2	-6.49×10^5	5.53×10^5
Pt- Sn^{2+} (w)	-9.67×10^4	-5.71×10	3.22×10^2	-6.49×10^5	5.53×10^5
Cy- Cr^{3+} (g)	-9.03×10^4	-0.91×10	3.01×10^2	-5.68×10^5	4.77×10^5
Cy- Cr^{3+} (w)	-2.33×10^5	-1.06×10^3	7.72×10^2	-2.27×10^6	2.04×10^6
Dp- Cr^{3+} (g)	-9.72×10^4	-1.14×10^2	3.23×10^2	-6.20×10^5	5.23×10^5
Dp- Cr^{3+} (w)	-2.24×10^5	-1.02×10^3	7.45×10^2	-2.12×10^6	1.90×10^6
Pt- Cr^{3+} (g)	-1.00×10^4	-7.83×10	3.35×10^2	-6.71×10^5	5.71×10^5
Pt- Cr^{3+} (w)	-1.90×10^5	-7.10×10^2	6.32×10^2	-1.72×10^6	1.53×10^6
Cy- Fe^{3+} (g)	-9.68×10^4	-1.34×10^2	3.22×10^2	-5.88×10^5	4.92×10^5
Cy- Fe^{3+} (w)	-2.24×10^5	-1.02×10^3	7.44×10^2	-2.10×10^6	1.88×10^6
Dp- Fe^{3+} (g)	-1.03×10^4	-7.85×10	3.45×10^2	-6.41×10^5	5.38×10^5
Dp- Fe^{3+} (w)	-2.31×10^5	-1.09×10^3	7.66×10^2	-2.16×10^6	1.92×10^6
Pt- Fe^{3+} (g)	-1.07×10^4	-1.60×10^2	3.56×10^2	-6.93×10^5	5.86×10^5
Pt- Fe^{3+} (w)	-1.52×10^5	-4.70×10^2	5.05×10^2	-1.19×10^6	1.04×10^6

ACN in plant systems lacking any electrons in d orbitals, and it is able to produce some metalloanthocyanins with the unfilled d or f orbitals [57]. Mg^{2+} was found to do function in the stereo chemical configurations of cyanidin, delphinidin and petunidin anthocyanins (Scheme 2, Figs. 1, 2). For discovering the impacts of Al^{3+} salt on food origin, anthocyanin was measured with the goal to better understanding blue color development of metallo-anthocyanin.

In calculations, Al^{3+} was identified to displace Mg^{2+} in anthocyanin- Mg^{2+} complexes, Cy based, and produces more stable complexes [55–57]. This M^{n+} has also even been estimated as a key to evaluate cyanidin,

delphinidin and petunidin in anthocyanin extracts from edible sources [55–57]. Similar to Mg^{2+} , Al^{3+} also lacks electrons in d orbitals but is trivalent when ionized.

In all pH, the frequency and dipole moment of anthocyanin-chelation were found to be significantly different with each metal treatment metallic cations of (Mg^{2+} , Al^{3+} , Ga^{3+} , Sn^{2+} , Cr^{3+} and Fe^{3+}) in Iranian Qara Qat fruit (Table 4). It has been seen that by increasing the pH, the frequency of [anthocyanin-metallic cations of (Mg^{2+} , Al^{3+} , Ga^{3+} , Sn^{2+} , Cr^{3+} and Fe^{3+})] cluster chelation in Iranian Qara Qat fruit increases between pH \approx 1.1–1.5 (Table 4, Fig. 6a, b).

Fig. 5 **a** Changes of Gibbs free energy(kcal/mol) of [ACN-Mg²⁺/Al³⁺/Ga³⁺/Sn²⁺/Cr³⁺/Fe³⁺] cluster chelation of Iranian Qara Qat fruit in two media of gas (g) and water (w) at 300 K, **b** Changes of enthalpy of reaction (ΔH_R) for formation of [ACN-Mg²⁺/Al³⁺/Ga³⁺/Sn²⁺/Cr³⁺/Fe³⁺] clusters in water medium

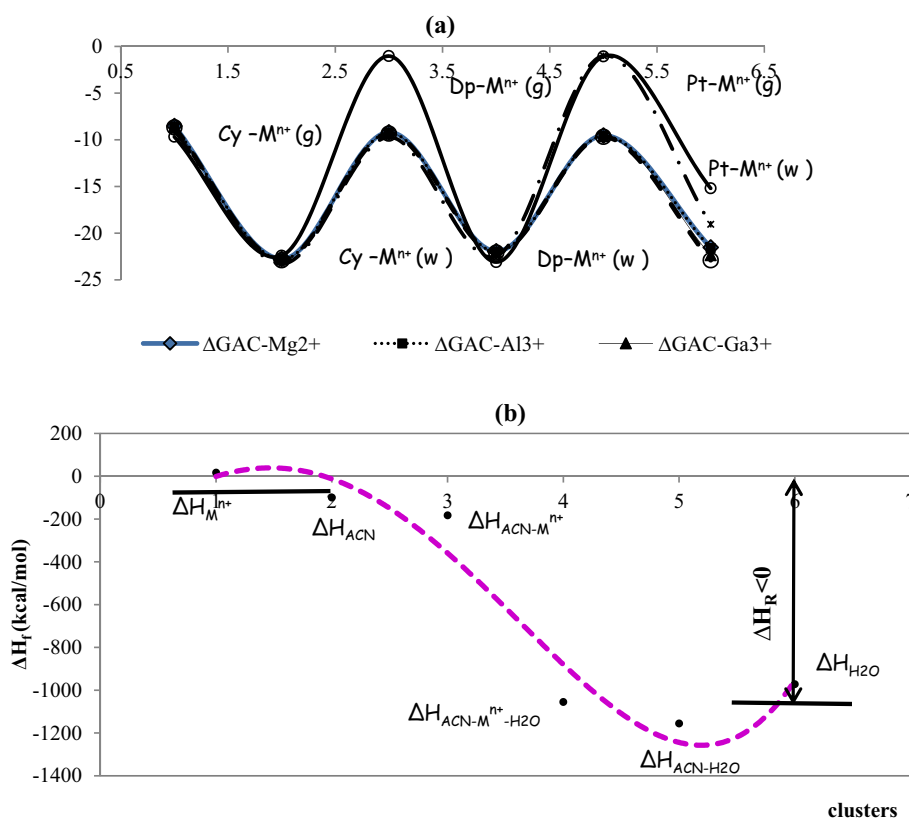


Table 3 The difference of ΔH_R through formation of [anthocyanin-metallic cations of (magnesium, aluminum, gallium, tin, chrome and iron)] cluster chelation in Iranian Qara Qat fruit

ΔH_R (ACN-M ⁿ⁺ -H ₂ O) (kcal/mol)											
Cy-Mg ²⁺	217.96	Cy-Al ³⁺	283.95	Cy-Ga ³⁺	288.58	Cy-Sn ²⁺	262.94	Cy-Cr ³⁺	199.19	Cy-Fe ³⁺	367.63
Dp-Mg ²⁺	382.21	Dp-Al ³⁺	453.46	Dp-Ga ³⁺	360.07	Dp-Sn ²⁺	387.29	Dp-Cr ³⁺	423.68	Dp-Fe ³⁺	319.20
Pt-Mg ²⁺	307.33	Pt-Al ³⁺	378.33	Pt-Ga ³⁺	278.95	Pt-Sn ²⁺	941.16	Pt-Cr ³⁺	575.31	Pt-Fe ³⁺	896.93

The maximum frequency of Al³⁺ treated acylated cyanidin was greater indicating the development of bluer colors, especially in higher pH with effects on their visible light absorbance (Fig. 6a, b).

Although we have little information about the interaction of anthocyanin with Cr³⁺, it is trivalent Mⁿ⁺ having electrons in d orbitals, where addition of Cr³⁺ to the ACN of this study was also found to induce frequency and absorbance of spectra. In all pH, the mean frequency of the anthocyanin of both sources was achieved to be various from one another with each metal cation.

Similar trends occurred with Cr³⁺, where the F_{max} of chelated cyanidin and delphinidin were greater while it has been indicated the maximum F of the anthocyanin with Cr³⁺ compared to Al³⁺ in chelation by cyanidin and petunidin.

Like Al³⁺, the impacts of Fe³⁺ chelated to anthocyanin were investigated to be better characterized to generate

some anthocyanin based blue colorations. Fe³⁺ is known to play an important role in many of the known pigment macromolecules [36].

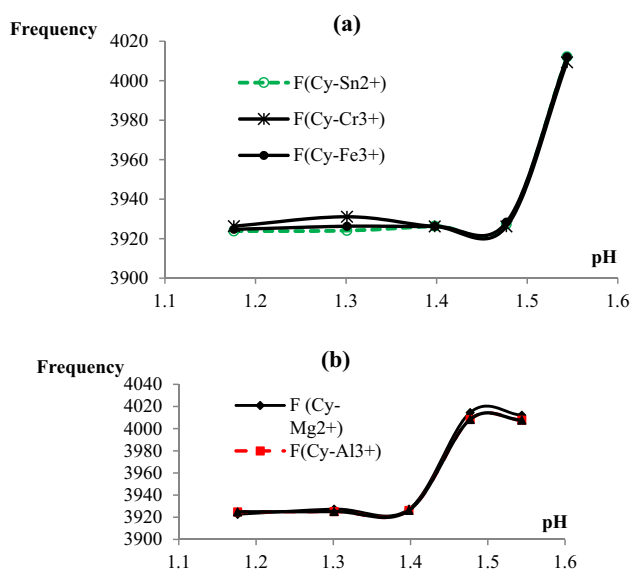
Those metalloanthocyanins with cyanidin chromophores need Fe³⁺ to generate blue hues, but those based on delphinidin chromophores can produce blue colors. So, it has been seen anthocyanin formed bonds with Fe³⁺ producing the highest shifted of frequency and absorbance compared to other metalloanthocyanins (Fig. 6a, b).

As it has been seen in Table 4, the physical properties of high frequency and dipole moment for anthocyanin-metal cation chelation of cyanidin-Al³⁺, delphinidin-Al³⁺, and petunidin-Al³⁺ have been calculated in weak acidic media extracted from the infrared computational method which has shown a high deviation of absorbance for [Al³⁺-chelation] of Dp pigment [55–57].

The frequency achieved of IR vibrational spectra has shown that the normal mode of the active sites due to

Table 4 Calculated dipole moment (D) (Debyes) and Frequency (F) (1/cm) of anthocyanin-metal chelation of cyanidin, delphinidin and petunidin in various pH using IR spectra

pH	Cy-Mg ²⁺		Cy-Al ³⁺		Cy-Ga ³⁺		Cy-Sn ²⁺		Cy-Cr ³⁺		Cy-Fe ³⁺	
	D	F	D	F	D	F	D	F	D	F	D	F
1.17	3.047	3922.7	18.655	3924.86	18.655	3924.86	4.027	3923.82	9.94	3926.3	7.384	3924.71
1.30	3.24	3927.39	16.739	3925.22	16.739	3925.22	3.104	3924.09	8.391	3931.09	5.914	3926.28
1.39	1.532	3927.39	16.351	3926.23	16.351	3926.23	6.931	3926.32	10.313	3926.2	7.149	3926.28
1.47	5.276	4014.5	13.82	4008.35	13.82	4008.35	3.081	3927.35	8.592	3926.21	4.695	3928.35
1.54	3.911	4012.12	6.687	4007.68	6.687	4007.68	7.005	4012.07	9.588	4009.28	6.471	4012.01
pH	Dp-Mg ²⁺		Dp-Al ³⁺		Dp-Ga ³⁺		Dp-Sn ²⁺		Dp-Cr ³⁺		Dp-Fe ³⁺	
	D	F	D	F	D	F	D	F	D	F	D	F
1.17	6.715	3926.53	1617.192	3925.8	18.783	3925.41	4.656	3923.57	9.042	3933.41	7.903	3767.49
1.30	3.676	3929.42	1745.149	3929.67	14.939	3927.6	3.513	3924.01	9.042	3933.41	1907.476	3945.54
1.39	22.597	5816.27	16.102	3929.62	12.995	3927.92	4.200	3925.99	6.406	3935.24	6.87	3928.67
1.47	4.913	3930.14	17.007	4015.05	2293.994	4040.77	2.271	4019.09	7.383	4017.84	5.545	4018.25
1.54	3.754	4018.29	16.865	4012.9	13.142	4014.13	3.899	4016.72	9.034	4015.4	6.379	4016.15
pH	Pt-Mg ²⁺		Pt-Al ³⁺		Pt-Ga ³⁺		Pt-Sn ²⁺		Pt-Cr ³⁺		Pt-Fe ³⁺	
	D	F	D	F	D	F	D	F	D	F	D	F
1.17	8.2	3925.49	22.838	3764.23	17.776	3926.05	5.342	3924.10	26.675	3767.37	8.2	3925.49
1.30	7.887	3925.48	1.2214	3930.1	16.375	3925.9	4.784	3924.54	9.775	3926.38	7.887	3925.48
1.39	6.593	3938.03	1935.273	7744.65	15.786	3936.28	4.213	3925.14	9.343	3944.92	6.593	3938.03
1.47	5.341	3941.18	16.276	3953.97	2473.38	3935.38	7.455	3925.49	6.893	3940.57	5.341	3941.18
1.54	6.517	3940.83	15.925	4013.69	12.817	4013.77	4.721	3925.73	6.207	3943.45	6.517	3940.83

**Fig. 6** Changes of Frequency (F) versus pH for **a** [cyanidin-metallic cations of (Sn²⁺, Cr³⁺ and Fe³⁺)] cluster chelation and **b** [cyanidin-metallic cations of (Mg²⁺, Al³⁺)] chelation in the weak acidic media by different concentrations of H⁺ at 300 K in Iranian Qara Qat fruit

anthocyanin-metal cation chelation of cyanidin-Al³⁺, delphinidin-Al³⁺, and petunidin-Al³⁺ in optimized weak acidic media approves the stability and color of these structures. The principal frequency vibrational modes have been illustrated based on the stability and color of various anthocyanin-metal cation chelation (Table 4).

In the next step, the atomic charge of indicated atoms in [anthocyanin-metallic cations of (Mg²⁺, Al³⁺, Ga³⁺, Sn²⁺, Cr³⁺ and Fe³⁺)] cluster chelation in Iranian Qara Qat fruit has been evaluated as the active parts of the molecules which play an important role for the electron charge transfer toward producing a range of various colors in water medium (Scheme 2, Figs. 1, 2, Table 5).

In Fig. 7a–c, it has been plotted the changes of atomic charge of labeled oxygen atoms and metal cations through optimized [anthocyanin-metallic cations of (Mg²⁺, Al³⁺, Ga³⁺, Sn²⁺, Cr³⁺ and Fe³⁺)] cluster chelation in Iranian Qara Qat fruit (Scheme 1, Figs. 1, 2); so, the results of Table 5 in a polar medium of water solution comparison to gas phase declare the stability and color of these compounds in the natural products of vegetables and fruits (Fig. 7a–c).

The outlook of Fig. 7a–c recommends the reason for existing observed various results of [anthocyanin-metallic cations of (Mg²⁺, Al³⁺, Ga³⁺, Sn²⁺, Cr³⁺ and Fe³⁺)] cluster chelation in Iranian Qara Qat fruit which are principally

Table 5 Atomic charge for Oxygen atoms in molecules of [anthocyanin-metallic cations of (Mg²⁺, Al³⁺, Ga³⁺, Sn²⁺, Cr³⁺ and Fe³⁺)] cluster chelation in Iranian Qara Qat fruit in different media of gas (g) and water (w)

Atom	Cy-Mg ²⁺	Cy-Mg ²⁺	Cy-Al ³⁺	Cy-Al ³⁺	Cy-Ga ³⁺	Cy-Ga ³⁺	Cy-Sn ²⁺	Cy-Sn ²⁺	Cy-Sn ²⁺	Cy-Cr ³⁺	Cy-Cr ³⁺	Cy-Fe ³⁺	Cy-Fe ³⁺
O10	-0.4070	-0.4252	-0.3274	-0.3639	-0.3685	-0.3752	-0.4715	-0.4947	0.0348	-0.0236	-0.1192	-0.1669	
O ⁺ 17	-0.1744	-0.1354	-0.1308	-0.1278	-0.1156	-0.1614	-0.1296	-0.1348	-0.1200	-0.1350	-0.1293	-0.1378	
O24	-0.2217	-0.2014	-0.1977	-0.1818	-0.1823	-0.2314	-0.2106	-0.2068	-0.1866	-0.2141	-0.2164	-0.2108	
O25	-0.2245	-0.2173	-0.2150	-0.2077	-0.2051	-0.2223	-0.2196	-0.2175	-0.2061	-0.2150	-0.2189	-0.2176	
O26	-0.2350	-0.2123	-0.2213	-0.2094	-0.2185	-0.2093	-0.2225	-0.2134	-0.2187	-0.2125	-0.2224	-0.2112	
O27	-0.3996	-0.3935	-0.3353	-0.3338	-0.3599	-0.3382	-0.4704	-0.4754	-0.0970	0.0752	-0.1466	-0.1350	
M ⁺ 31	0.7701	0.7624	-0.0025	-0.0201	-0.0315	0.7577	0.9251	0.9424	-0.8628	-0.4498	0.0273	0.0766	
Atom	Dp-Mg ²⁺ (g)	Dp-Mg ²⁺ (w)	Dp-Al ³⁺ (g)	Dp-Al ³⁺ (w)	Dp-Ga ³⁺ (g)	Dp-Ga ³⁺ (w)	Dp-Sn ²⁺ (g)	Dp-Sn ²⁺ (w)	Dp-Cr ³⁺ (g)	Dp-Cr ³⁺ (w)	Dp-Fe ³⁺ (g)	Dp-Fe ³⁺ (w)	
O9	-0.3774	-0.3932	-0.2871	-0.3264	-0.3314	-0.5631	-0.2991	-0.4727	0.0678	0.0050	0.0968	-0.1422	
O ⁺ 16	-0.1753	-0.1361	-0.1314	-0.1285	-0.1163	-0.1313	-0.1322	-0.1340	-0.1319	-0.1350	-0.1311	-0.1362	
O23	-0.2200	-0.1979	-0.2037	-0.1868	-0.1833	-0.1803	-0.2117	-0.2021	-0.2192	-0.2102	-0.2463	-0.2069	
O24	-0.2242	-0.2074	-0.2165	-0.1995	-0.2054	-0.2018	-0.2194	-0.2082	-0.2185	-0.2054	-0.2302	-0.2071	
O25	-0.2345	-0.2157	-0.2211	-0.2138	-0.2184	-0.2149	-0.2223	-0.2166	-0.2224	-0.2158	-0.2269	-0.2169	
O26	-0.4020	-0.3970	-0.3313	-0.3316	-0.3504	-0.6333	-0.3269	-0.4667	0.0478	0.0634	0.0469	-0.1260	
O30	-0.2124	-0.2107	-0.1690	-0.1922	-0.1812	-0.1867	-0.2041	-0.2030	-0.2076	-0.2105	-0.2433	-0.2131	
M ⁺ 32	0.7645	0.7602	0.0063	0.0385	-0.0575	0.6460	0.5521	0.9448	-0.4936	-0.4268	0.2444	0.0444	
Atom	Pt-Mg ²⁺ (g)	Pt-Mg ²⁺ (w)	Pt-Al ³⁺ (g)	Pt-Al ³⁺ (w)	Pt-Ga ³⁺ (g)	Pt-Ga ³⁺ (w)	Pt-Sn ²⁺ (g)	Pt-Sn ²⁺ (w)	Pt-Cr ³⁺ (g)	Pt-Cr ³⁺ (w)	Pt-Fe ³⁺ (g)	Pt-Fe ³⁺ (w)	
O ⁺ 7	-0.1762	-0.1361	-0.1322	-0.1285	-0.1249	-0.1317	-0.1220	-0.1220	-0.1324	-0.1329	-0.1327	-0.1367	
O17	-0.3811	-0.3989	-0.2934	-0.3328	-0.5658	-0.5731	-0.3152	-0.3152	0.0460	0.0329	-0.1157	-0.1279	
O18	-0.4015	-0.3940	-0.3315	-0.3287	-0.6413	-0.6332	-0.3396	-0.3396	0.0224	0.0389	-0.1271	-0.1769	
O19	-0.2200	-0.2004	-0.2031	-0.1884	-0.1833	-0.1888	-0.2148	-0.2148	-0.2184	-0.2165	-0.1271	-0.2136	
O20	-0.2345	-0.2168	-0.2211	-0.2146	-0.2203	-0.1940	-0.2256	-0.2148	-0.2228	-0.2152	-0.2230	-0.2039	
O21	-0.2245	-0.2208	-0.2168	-0.2123	-0.2111	-0.2155	-0.2225	-0.2225	-0.2194	-0.2188	-0.2202	-0.2194	
O30	-0.1520	-0.1505	-0.1100	-0.1314	-0.1202	-0.1263	-0.1472	-0.1472	-0.1503	-0.1565	-0.1532	-0.1529	
M ⁺ 35	0.7656	0.7630	0.0040	0.0304	0.6476	0.6472	0.5786	0.5786	-0.4207	-0.4231	0.0166	0.0958	

linked to the position of active sites of labeled oxygen atoms and metal cations in these molecules which move the charge of electrons in aromatic cyclic chains because of water polar medium in contrast to gas phase and the lowest deviation for two media of water and gas has been indicated for anthocyanin-Mg²⁺ (Fig. 7 a-c).

In fact, the spin density and partial charges have been obtained by fitting the electrostatic potential to fixed charge of O₁₇⁺, O₁₆⁺, and O₇⁺ cations for cyanidin-Mⁿ⁺ (31), delphinidin-Mⁿ⁺ (32) and petunidin-Mⁿ⁺ (35), respectively (Table 5, Fig. 7a-c); therefore, the electrophilic groups of cyanidin, delphinidin anthocyanin pigments conduct us to find the reason for the activity and the stability of these structures in the natural products.

5 Conclusion

In this study, the anthocyanins of cyanidin (Cy), delphinidin (Dp) and petunidin (Pt) with a large chelation in the active zone of these structures by metallic cations of (Mg²⁺, Al³⁺, Ga³⁺, Sn²⁺, Cr³⁺ and Fe³⁺) metallic cations make a variety range of colors under acidic pH; as divalent Mg²⁺ has shown various physicochemical properties considering its optimized geometry optimization as the bond length of oxygen—Mg²⁺ ≈ (1.9 Å) and the bond angle of oxygen—Mg²⁺—oxygen ≈ (112°) while it has been indicated the bond length of oxygen—M³⁺ ≈ (1.8 Å) and bond angle of oxygen—M³⁺—oxygen ≈ (120°) for trivalent metallic cations of (Mg²⁺, Al³⁺, Ga³⁺, Sn²⁺, Cr³⁺ and Fe³⁺) metallic cations with more electron rich metal ions caused shifts and hue changes in the stability of color and structure.

Moreover, we have found that [anthocyanin-metallic cations of (Mg²⁺, Al³⁺, Ga³⁺, Sn²⁺, Cr³⁺ and Fe³⁺)] cluster chelation is based on the axes of active zones of specified oxygen atoms and metallic cations in these complexes

which shift the electronic charges in aromatic cyclic chains because of water dielectric constant in contrast to gas medium. The spin density and partial charges have been gained by establishing the electrostatic potential to fix charge of O₁₇⁺, O₁₆⁺, and O₇⁺ cations for cyanidin-Mⁿ⁺ (31), delphinidin-Mⁿ⁺ (32) and petunidin-Mⁿ⁺ (35), respectively based on the electrophilic groups of cyanidin, delphinidin and petunidin of anthocyanin colorful pigments which show the activity and the stability of these compounds toward the natural material. Generally, anthocyanin is capable to chelate the Mⁿ⁺ through indicating the shift in their frequency and absorbance spectra which are affected by several factors including the anthocyanin structure, pH which is the important environmental factor in the expressed color of the solutions, and also the atomic configuration of the metallic cations.

Divalent Mg²⁺ was found to impact anthocyanin minimally with raising electron density in different pH; Sn²⁺ ≈ Fe³⁺ ≈ Ga³⁺ > Al³⁺ > Cr³⁺ > Mg²⁺

Using Beer Lambert law on [anthocyanin-metallic cations of (Mg²⁺, Al³⁺, Ga³⁺, Sn²⁺, Cr³⁺ and Fe³⁺)] cluster chelation of cyanidin, delphinidin, and petunidin pigments in Iranian Qara Qat fruit using theoretical methods illustrates absorbance factor in two media of gas and water and then unravels the stabilization energy and geometry which have been impacted by IR theoretical modeling toward the thermodynamic properties and the electronic structural of optimized [anthocyanin-metallic cations of (Mg²⁺, Al³⁺, Ga³⁺, Sn²⁺, Cr³⁺ and Fe³⁺)] cluster chelation in Iranian Qara Qat fruit resulting of metal chelation.

The results have exhibited that such extrapolation Schemes 1, 2, 3 and 4 significantly overestimate [anthocyanin-metallic cations of (Mg²⁺, Al³⁺, Ga³⁺, Sn²⁺, Cr³⁺ and Fe³⁺)] cluster chelation in Iranian Qara Qat fruit by sharp parts of electrophilic molecules in weak acidic media with different concentrations of H⁺ which are the most active particles at the applied compounds in this project.

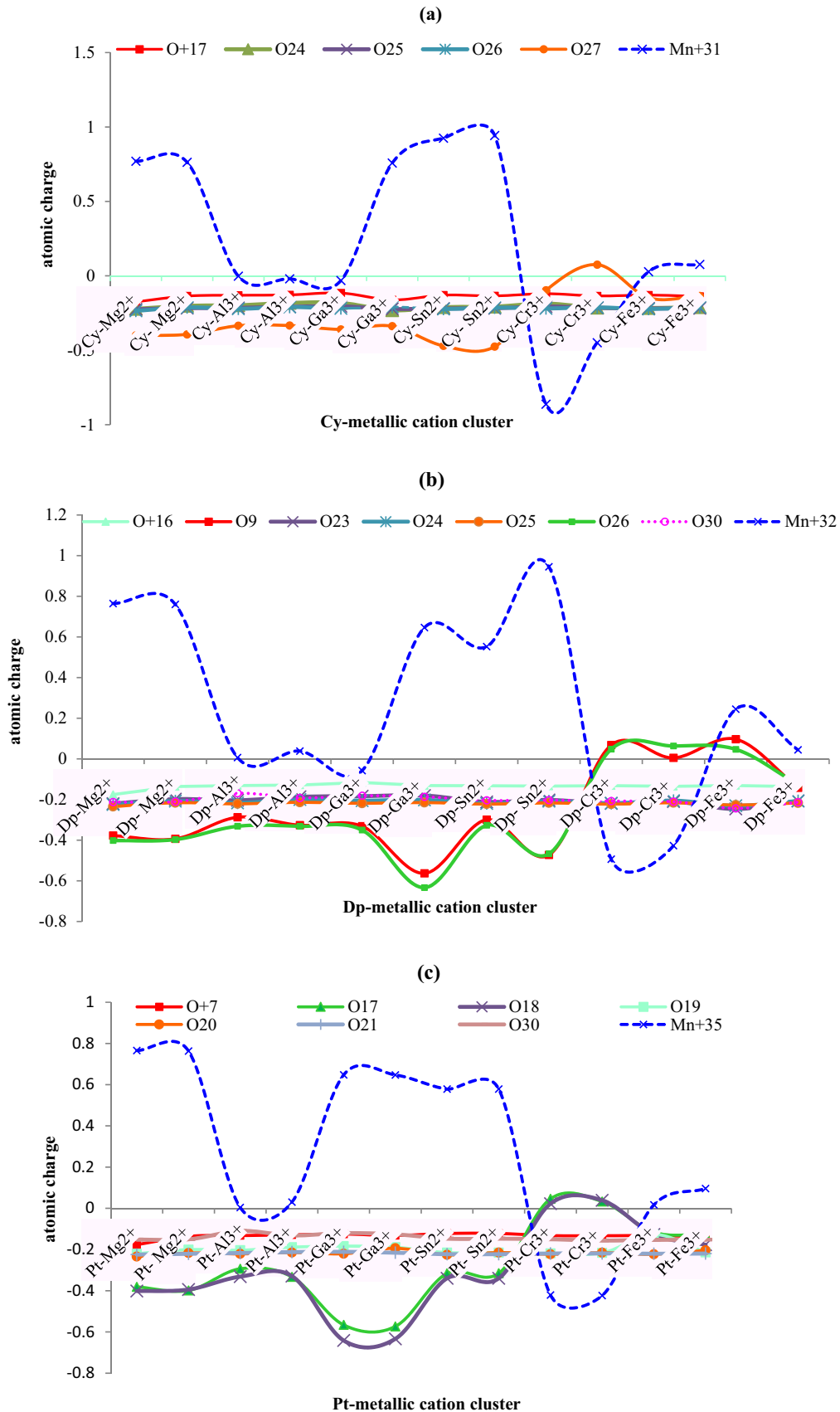


Fig. 7 Comparison of atomic charge versus labeled oxygen atoms and metal cations through optimized **a** [cyanidin-metallic cations of (Mg^{2+} , Al^{3+} , Ga^{3+} , Sn^{2+} , Cr^{3+} and Fe^{3+})], **b** [delphinidin-metallic cations of (magnesium, aluminum, gallium, tin, chrome and iron)] and **c** [petunidin-metallic cations of (magnesium, aluminum, gallium, tin, chrome and iron)] cluster chelation of Iranian Qara Qat fruit in two media of gas and water

Declarations

Conflict of interest The authors declare that they have no competing interests.

Open Access This article is licensed under a Creative Commons Attribution 4.0 International License, which permits use, sharing, adaptation, distribution and reproduction in any medium or format, as long as you give appropriate credit to the original author(s) and the source, provide a link to the Creative Commons licence, and indicate if changes were made. The images or other third party material in this article are included in the article's Creative Commons licence, unless indicated otherwise in a credit line to the material. If material is not included in the article's Creative Commons licence and your intended use is not permitted by statutory regulation or exceeds the permitted use, you will need to obtain permission directly from the copyright holder. To view a copy of this licence, visit <http://creativecommons.org/licenses/by/4.0/>.

References

- Quina FH, Bastos EL (2018) Chemistry inspired by the colors of fruits, flowers and wine. *An Acad Bras Cienc* 90:681
- Castaneda-Ovando A, Pacheco-Hernandez ML, Paez-Hernandez ME, Rodriguez JA, Galan-Vidal CA (2009) Chemical studies of anthocyanins: a review. *Food Chem* 113:859
- Pina F, Oliveira J, Freitas V (2015) Anthocyanins and derivatives are more than flavylium cations. *Tetrahedron* 71:3107
- Castañeda-Ovando A, de Lourdes Pacheco-Hernández M, Páez-Hernández E et al (2009) Chemical studies of anthocyanins: a review. *Food Chem* 113(4):859–871
- Seeram NP, Momin RA, Nair MG et al (2001) Cyclooxygenase inhibitory and antioxidant cyanidin glycosides in cherries and berries. *Phytomedicine* 8(5):362–369
- Cevallos-Casals BA, Cisneros-Zevallos L (2003) Stoichiometric and kinetic studies of phenolic antioxidants from Andean purple corn and red-fleshed sweetpotato. *J Agric Food Chem* 51(11):3313–3319
- Katsumoto Y, Fukuchi-Mizutani M, Fukui Y et al (2007) Engineering of the rose flavonoid biosynthetic pathway successfully generated blue-hued flowers accumulating delphinidin. *Plant Cell Physiol* 48(11):1589–1600
- Bąkowska-Barczak A (2005) Acylated anthocyanins as stable, natural food colorants—a review. *Pol J Food Nutr Sci* 14/55(2):107–116
- Robinson GM, Robinson R (1932) A survey of anthocyanins II. *Biochemical J* 6(5):1647
- Jaakola L (2013) New insights into the regulation of anthocyanin biosynthesis in fruits. *Trends Plant Sci* 18(9):477–483
- Olsson ME, Gustavsson KE, Andersson S, Nilsson Å, Duan RD (2004) Inhibition of cancer cell proliferation in vitro by fruit and berry extracts and correlations with antioxidant levels. *J Agric Food Chem* 52:7264–7271
- Hassan HA, Abdel-Aziz AF (2010) Evaluation of free radical-scavenging and anti-oxidant properties of black berry against fluoride toxicity in rats. *Food Chem Toxicol* 48:1999–2004
- Duthie SJ (2007) Berry phytochemicals, genomic stability and cancer: evidence for chemoprotection at several stages in the carcinogenic process. *Mol Nutr Food Res* 51(6):665–674
- Ardalan T, Ardalan P, Monajjemi M (2014) Nano theoretical study of a C16 cluster as a novel material for vitamin C carrier. *Fuller Nanotub Carbon Nanostruct* 22(8):687–708
- Taylor LP, Grotewold E (2005) Flavonoids as developmental regulators. *Curr Opin Plant Biol* 8:317–323
- Peer WA, Murphy AS (2007) Flavonoids and auxin transport: modulators or regulators? *Trends Plant Sci* 12:556–563
- Monajjemi M, Ahmadianarog M (2014) Carbon nanotube as a deliver for sulforaphane in Broccoli vegetable in point of nuclear magnetic resonance and natural bond orbital specifications. *J Comput Theor Nanosci* 11(6):1465–1471
- Hudson EA, Dinh PA, Kokubun T, Simmonds MS, Gescher A (2000) Cancer epidemiology. *Biomarkers Prev* 9:1163–1170
- Harborne JB (1998) Phenolic compounds. In: Harborne JB (ed) *Phytochemical methods, a guide to modern techniques of plant analysis*, 3rd edn. Chapman & Hall, New York, pp 66–74
- Wenzel J, Wang L, Horcasitas S, Warburton A, Constine S, Kjellson A, Cussans K, Ammerman M, Samaniego CS (2020) Influence of supercritical fluid extraction parameters in preparation of black chokeberry extracts on total phenolic content and cellular viability. *Food Sci Nutr* 8(7):3626–3637
- Heredia FJ, Francia-Aricha EM, Rivas-Gonzalo JC, Vicario IM, Santos-Buelga C (1998) Chromatic characterization of anthocyanins from red grapes—I. pH effect. *Food Chem* 63:491–498
- Ahmadiani N, Robbins RJ, Collins TM et al (2014) Anthocyanins contents, profiles, and color characteristics of red cabbage extracts from different cultivars and maturity stages. *J Agric Food Chem* 62(30):7524–7531
- Sidor A, Gramza-Michałowska A (2019) Black Chokeberry *Aronia melanocarpa* L.-a qualitative composition, phenolic profile and antioxidant potential. *Molecules* 24(20):3710
- Koss-Mikołajczyk I, Kusznierevicz B, Bartoszek A (2019) The relationship between phytochemical composition and biological activities of differently pigmented varieties of berry fruits; comparison between embedded in food matrix and isolated anthocyanins. *Foods* 8(12):646
- Borkowski T, Szymusiak H, Gliszczynska-Swiglo A, Tyrakowska B (2005) The effect of 3-O-β-glucosylation on structural transformations of anthocyanidins. *Food Res Int* 38:1031–1037
- Freitas AA, Shimizu K, Dias LG, Quina FH (2007) A computational study of substituted flavylium salts and their quinonoid conjugate-bases: S0 → S1 electronic transition, absolute pKa and reduction potential calculations by DFT and semiempirical methods. *J Braz Chem Soc* 18(8):1537–1546
- Sigurdson GT, Tang P, Giusti MM (2017) Natural colorants: food colorants from natural sources. *Annu Rev Food Sci Technol* 8:261
- Freitas AA, Dias LG, Maçanita AAL, Quina FH (2011) Substituent effects on the pH-dependent multiequilibria of flavylium salt analogs of anthocyanins: substituent effects on anthocyanin analogs. *J Phys Org Chem* 24:1201
- Ananga A, Georgiev V, Ochieng J, Phills B, Tsovala V (2013) Production of anthocyanins in grape cell cultures: a potential source of raw material for pharmaceutical, food, and cosmetic industries. In: Puljuha D, Sladonja B (eds) *The Mediterranean genetic code—grapevine and olive*, 1st edn. InTech, Rijeka, Croatia, pp 247–288

30. Glińska S, Bartczak M, Oleksiak S, Wolska A, Gabara B, Posmyk M, Janas K (2007) Effects of anthocyanin-rich extract from red cabbage leaves on meristematic cells of *Allium cepa* L. roots treated with heavy metals. *Ecotoxicol Environ Saf* 68(3):343–350
31. Schreiber HD, Swink AM, Godsey TD (2010) The chemical mechanism for Al^{3+} complexing with delphinidin: a model for the bluing of hydrangea sepals. *J Inorg Biochem* 104(7):732–739
32. Dangles O, Elhabiri M, Brouillard R (1994) Kinetic and thermodynamic investigation of the aluminium-anthocyanin complexation in aqueous solution. *J Chem Soc Perkin Trans 2*(12):2587
33. Cabrita L, Fossen T, Andersen ØM (2000) Colour and stability of the six common anthocyanidin 3-glucosides in aqueous solutions. *Food Chem* 68(1):101–107
34. Fossen T, Cabrita L, Andersen OM (1998) Colour and stability of pure anthocyanins influenced by pH including the alkaline region. *Food Chem* 63(4):435–440
35. Buchweitz M, Carle R, Kammerer DR (2012) Bathochromic and stabilizing effects of sugar beet pectin and an isolated pectic fraction on anthocyanins exhibiting pyrogallol and catechol moieties. *Food Chem* 135(4):3010–3019
36. Yoshida K, Mori M, Kondo T (2009) Blue flower color development by anthocyanins: from chemical structure to cell physiology. *Nat Prod Rep* 26(7):884–915
37. Frisch MJ, Trucks GW, Schlegel HB, Scuseria GE, Robb MA, Cheeseman JR, Scalmani G, Barone V, Mennucci B, Petersson GA, Nakatsuji H, Caricato M, Li X, Hratchian HP, Izmaylov AF, Bloino J, Zheng G, Sonnenberg JL, Hada M, Ehara M, Toyota K, Fukuda R, Hasegawa J, Ishida M, Nakajima T, Honda Y, Kitao O, Nakai H, Vreven T, Montgomery JA Jr, Peralta JE, Ogliaro F, Bearpark M, Heyd JJ, Brothers E, Kudin KN, Staroverov VN, Kobayashi R, Normand J, Raghavachari K, Rendell A, Burant JC, Iyengar SS, Tomasi J, Cossi M, Rega N, Millam JM, Klene M, Knox JE, Cross JB, Bakken V, Adamo C, Jaramillo J, Gomperts R, Stratmann RE, Yazyev O, Austin AJ, Cammi R, Pomelli C, Ochterski JW, Martin RL, Morokuma K, Zakrzewski VG, Voth GA, Salvador P, Dannenberg JJ, Dapprich S, Daniels AD, Farkas O, Foresman JB, Ortiz JV, Cioslowski J, Fox DJ (2010) Gaussian 09, Revision B.01. Gaussian Inc., Wallingford
38. Martin K, Andrew McCammon J (2002) Erratum: Molecular dynamics simulations of biomolecules. *Nat Struct Biol* 9:788
39. Wilfred F, Gunsteren V, Berendsen HJC (1990) Computer simulation of molecular dynamics: methodology, applications, and perspectives in chemistry. *Angew Chem Int Ed English* 29(9):992–1023
40. Ni W, Li G, Zhao J, Cui J, Wang R, Gao Z, Liu Y (2018) Use of Monte Carlo simulation to evaluate the efficacy of tigecycline and minocycline for the treatment of pneumonia due to carbapenemase-producing *Klebsiella pneumoniae*. *Infect Dis (Lond)* 50(7):507–513
41. Andrews CW, Wisowaty J, Davis AO, Crouch RC, Martin GE (1995) Molecular modeling, NMR spectroscopy, and conformational analysis of 3',4'-anhydrovinblastine. *J Heterocycl Chem* 32(3):1011–1017
42. Monajjemi M, Honarparvar B, Nasser SM, Khaleghian M (2009) NQR and NMR study of hydrogen bonding interactions in anhydrous and monohydrated guanine cluster model: a computational study. *J Struct Chem* 50(1):67–77
43. Monajjemi M, Ghiasi R, Sadjadi MS (2003) Metal-stabilized rare tautomers: N4 metalated cytosine (M = Li, Na, K, Rb and Cs), theoretical views. *Appl Organomet Chem* 17(8):635–640
44. Wilfred F, Berendsen HJC (1990) Computer simulation of molecular dynamics methodology, applications, and perspectives in chemistry. *Angew Chem Int Ed English* 29:992–1023
45. Karplus M, Petsko GA (1990) Molecular dynamics simulations in biology. *Nature* 347:631–639
46. Cohen G, Eisenberg H (1968) Deoxyribonucleate solutions: Sedimentation in a density gradient, partial specific volumes, density and refractive index increments, and preferential interactions. *Biopolymers* 6:1077
47. Beak P, Covington JB, Smith SG, White JM, Zeiger JM (1980) Displacement of protomeric equilibria by self-association: hydroxypyridine-pyridone and mercaptopyridine-thiopyridone isomer pairs. *J Org Chem* 45:1354
48. Kirkwood JG (1934) On the theory of strong electrolyte solutions. *J Chem Phys* 2:767
49. Kirkwood JG (1939) The dielectric polarization of polar liquids. *J Chem Phys* 7:911
50. Onsager L (1936) Electric moments of molecules in liquids. *J Am Chem Soc* 58:1486
51. Wong MA, Frisch MJ, Wiberg KB (1991) Solvent effects. 1. The mediation of electrostatic effects by solvents. *J Am Chem Soc* 113:4776
52. Wong MA, Frisch MJ, Wiberg KB (1992) Solvent effects. 2. Medium effect on the structure, energy, charge density, and vibrational frequencies of sulfamic acid. *J Am Chem Soc* 114:523
53. van der Kamp MW, Mulholland AJ (2013) Combined quantum mechanics/molecular mechanics (QM/MM) methods in computational enzymology. *Biochemistry* 52(16):2708–2728
54. Gadda G, Sobrado P (2018) Kinetic solvent viscosity effects as probes for studying the mechanisms of enzyme action. *Biochemistry* 57(25):3445–3453
55. Kunsági-Máté S, Ortmann E, Kollár L, Szabó K, Nikfardjam MP (2008) Effect of ferrous and ferric ions on copigmentation in model solutions. *J Mol Struct* 891(1–3):471–474
56. Estévez L, Otero N, Mosquera RA (2011) Molecular structure of cyanidin metal complexes: Al(III) versus Mg(II). *Theoret Chem Acc* 128(4):485–495
57. Mason RP (2013) Chemical thermodynamics and metal (loid) complexation in natural waters. In: Mason RP (ed) Trace metals in aquatic systems, 1st edn. Blackwell Publishing (John Wiley & Sons Ltd.), Chichester, West Sussex, pp 49–123

Publisher's Note Springer Nature remains neutral with regard to jurisdictional claims in published maps and institutional affiliations.